Shear and tensile relaxation behaviour in oriented linear polyethylene

A. G. Gibson*, S. A. Jawad†, G. R. Davies and I. M. Ward
Department of Physics, University of Leeds, Leeds, LS2 9JT, UK
(*Received* 11 *June* 1981)

The dynamic shear behaviour of oriented linear polyethylene has been studied with particular reference to previous studies of the dynamic tensile modulus. First, it has been shown that the increase in the −50°C plateau shear modulus with draw ratio can be understood on a Takayanagi-type model in terms of an increase in crystal continuity. The crystal continuity is estimated from the longitudinal crystal thickness and the long period on the basis of the random crystalline bridge model. At a similar level of sophistication it is also possible to explain the cross-over in the ranking of samples of increasing draw ratio with change of temperature. The dynamic mechanical behaviour is then considered in terms of a simple extension of this Takayanagi model in which crystalline sequences which span two or more adjacent lamellae are regarded as the fibre phase in a short fibre composite. It can be shown that this model gives a satisfactory prediction of the changes in dynamic tensile modulus and loss with temperature, for a range of samples with different degrees of crystal continuity.

Keywords Mechanical behaviour; relaxation; polyethylene; linear; oriented, shear; tensile

INTRODUCTION

In a number of previous publications[1-4] we have presented our interpretation of the dynamic tensile behaviour, the thermal expansion and the thermal conductivity of ultra-oriented LPE in terms of present knowledge of the structure of these materials. In this paper, the dynamic shear behaviour is presented and its relationship to dynamic tensile behaviour discussed.

First, it will be shown that the increase in the −50°C plateau shear modulus with draw ratio can be understood on the basis of the Takayanagi model in terms of the increase in crystal continuity. At a similar level, it is also possible to explain the cross-over in the ranking of different samples with change of temperature.

The dynamic shear data are then combined with dynamic tensile data to examine the validity of a simple model, in which the oriented polymer is regarded as a short fibre composite, the fibre phase consisting of crystalline sequences which span two or more adjacent lamellae. It will be shown that the model provides a consistent understanding of the changes in dynamic modulus and loss with temperature, for a range of samples with different degrees of crystal continuity.

EXPERIMENTAL

Preparation of samples

Oriented rods of linear polyethylene were prepared by hydrostatic extrusion at 100°C of solid cylindrical billets through a conical die to a final bore diameter of 2.5 mm. Deformation ratios in the range 5 to 25 were used. Further details of the hydrostatic extrusion process are given in previous publications[1,5]. In this paper we describe results for Rigidex 50, a linear homopolymer manufactured by BP Chemicals International Ltd, which has weight-average and number-average molecular weights of 101 450 and 6180 respectively.

Characterization of samples

Wide angle X-ray diffraction of all samples showed that the crystallite orientation was in all cases very high. We have also made use of X-ray diffractometry studies, which have been reported previously[6], to provide estimates of $\bar{D}_{002}$, the average crystalline dimension of the c direction. These results, together with values of the long period L, determined by small angle X-ray diffraction, have been used to provide a measure of crystalline continuity.

Mechanical measurements

The dynamic shear measurements were undertaken at 1 Hz using a free oscillation torsion pendulum of the counter balanced inertia arm type, similar to that adopted by Heijboer and co-workers[7]. In this equipment the sample is rigidly clamped at its lower end to the base of the apparatus and to a rod supported by the counter balance at the upper end. A beam of light is reflected from a mirror attached to the upper clamp, such that it falls on a split photocell. The photocell assembly then follows the deflected light beam and a pen traces the oscillations on a chart recorder. The shear modulus is calculated from the frequency and tan δ from the logarithmic decrement of the free oscillations.

It has been shown that end effects due to localized stress concentrations near the grips can significantly affect the results of torsional measurements on highly anisotropic materials[8]. We therefore took especial care to reduce these effects to a negligible order of magnitude by ensuring that the aspect ratio of the samples was very high, a value of 40:1 (length between clamps/diameter) being adopted. As already indicated the oriented samples were of circular cross-section. The isotropic sample was of rectangular cross-section and was machined from an injection moulded rod. The machining operation was performed to

* Now at Metallurgy and Materials Science, University of Liverpool, UK
† Now at Department of Physics, University of United Arab Emirates

0032-3861/82/030349-10$03.00

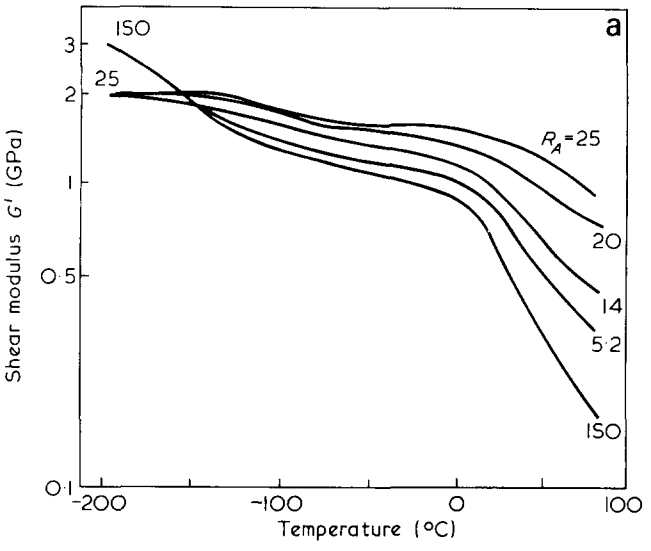

Figure 1a The dynamic shear modulus G' as a function of temperature for samples of different draw ratio (R_A)

remove the surface layers of the rod, and hence eliminate any possible effects due to oriented surface layers. The rectangular cross-section was dictated solely by convenience of the machining operation and is not expected to have any significant effect on the results.

Measurements were carried out in the temperature region from ambient down to −150°C by blowing cold nitrogen gas into a thermally insulated chamber surrounding the samples. An additional measurement at −196°C was made possible by introducing liquid nitrogen into the chamber. Temperatures between ambient and 100°C were achieved by passing heated nitrogen into the chamber.

There is evidence from previous studies that these highly oriented samples are thermally stable up to at least 100°C, and only at higher temperatures do structural changes due to recrystallization and lamellar thickening occur. To avoid any changes due to such effects we therefore selected 100°C as the maximum temperature of measurement and as a further precaution all samples were held at this temperature for at least 20 min before measurements commenced.

For measurements made in the low temperature γ relaxation region, care was taken to reduce the temperature fairly slowly over a period of one hour or more, since it is known that rapid quenching can result in spurious time-dependent effects on tan δ, which have been attributed to the relaxation of localized thermal strains at a morphological level.

The dynamic tensile measurements have been reported in our previous publication[1], where full details are given. Dynamic three point bend tests were undertaken at 3.6 Hz on samples of very high aspect ratio, to minimize shear and end effects. As in the case of the torsion measurements, especial care was taken to change the sample temperature slowly, so as to eliminate spurious effects on the mechanical behaviour.

RESULTS

Figure 1a shows the storage modulus, G', as a function of temperature for the extruded and isotropic samples. All sets of curves show the general features observed previously: the two plateaux, below −196°C and at −50°C, and the drop in modulus at higher temperatures due to the onset of the α-relaxation. However the change in G' with increasing deformation ratio is much less spectacular than the changes in the Young's modulus, E', and the curves tend much more to approach a single envelope at high deformation ratios. The results for E' and $\tan\delta_E$ have been reproduced in this paper in *Figures 5a* and *5b*, where they are shown in order to enable a comparison with the theoretical modelling. The amount by which G' drops with temperature, both in the low temperature (γ) region, and the high temperatures, decreases considerably with increasing deformation ratio. Indeed the curve for the $\lambda = 25$ sample shows an overall degree of temperature dependence which is remarkably low for a semicrystalline polymer. The cross-over between the G' values for isotropic and oriented samples in the γ-region is particularly noteworthy and its significance will be discussed later.

The curves for the loss factor, $\tan\delta_G$, shown in *Figure 1b* also show the α and γ relaxations observed previously, and it is remarkable that although the intensity of these relaxations, as measured by tanδ, decreases with increasing deformation ratio, their shape and position changes very little. In all these respects, there is again a close similarity with the previous measurements of $\tan\delta_E$.

DISCUSSION

The structure of ultra-oriented LPE

It has been shown[1] that the dynamic tensile behaviour of drawn and extruded LPE could be very well explained in terms of a model for the structure in which the lamellar stacks characteristic of low draw material become increasingly linked by randomly arranged crystalline bridges as the draw ratio is increased. This model is consistent with the very high crystallite orientation for all drawn material, the retention of a two point small angle X-ray diffraction pattern which diminishes in intensity with increasing draw, and the observation that the average crystal length increases to a value of ~500 Å for

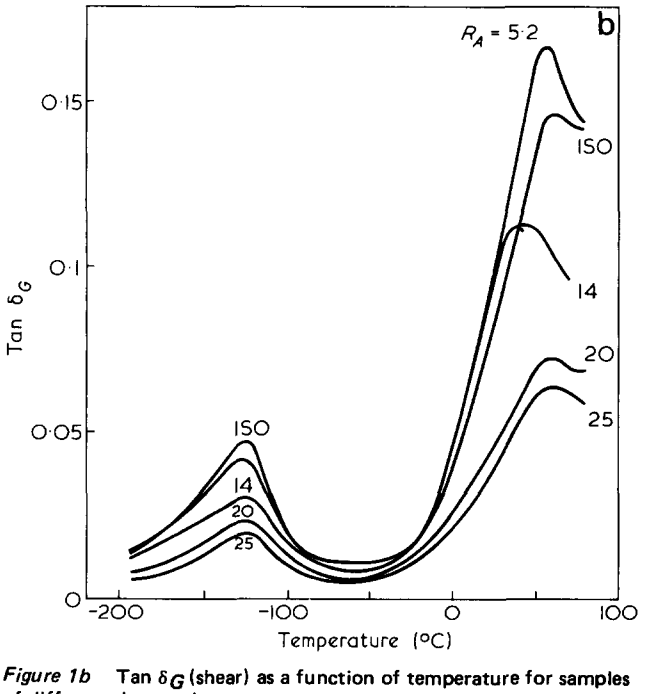

Figure 1b Tan δ_G (shear) as a function of temperature for samples of different draw ratio

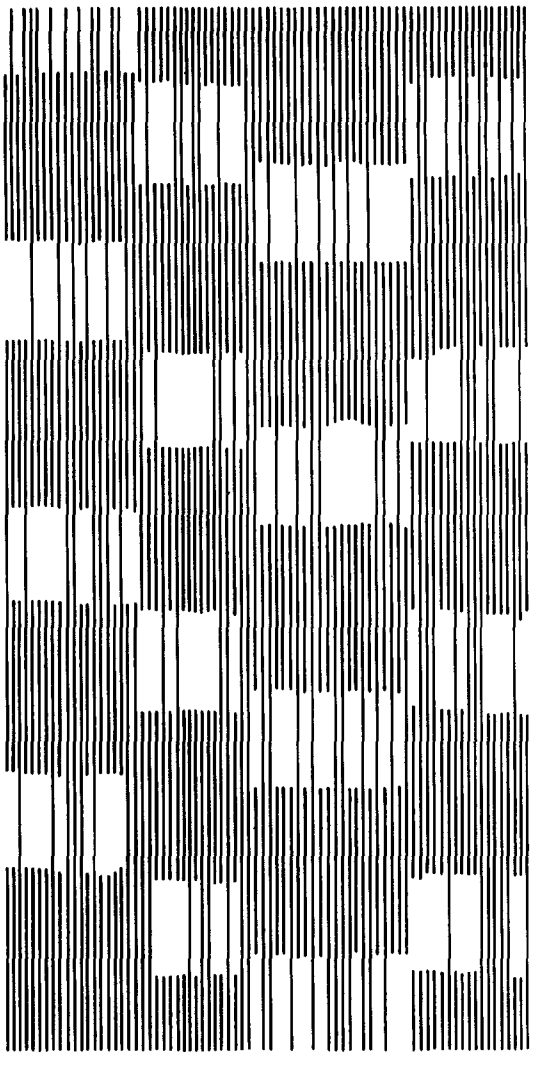

Figure 2 A schematic structure of ultra-oriented polyethylene showing lamellae linked by intercrystalline bridges

the mostly highly drawn material (cf. constant long period ~200 Å).

To make the quantitative connection between the dynamic tensile behaviour and structure it was considered that the degree of crystalline continuity can be related to a single parameter p which defines the probability that a crystalline sequence traverses the disordered regions to link two adjacent lamellae. The lengths of the crystalline sequences (i.e. the crystal length distribution) are then determined by statistics exactly analogous to those for a stepwise condensation polymerization. p can be determined from measurements of the integral breadth of the (002) reflection which gives the weight average crystalline sequence length in c-axis direction, $\bar{D}_{002}$, and the small angle X-ray long period L. Even for the highest deformation ratio (~30) (obtainable by drawing) it was found that p did not exceed 0.4, which implies that the majority of the crystalline bridges only span adjacent lamellae. A diagrammatic representation of the structure is shown in *Figure 2* and the essential correctness of the model has recently been confirmed by dark field electron microscopy[9] and nitric acid etching followed by gel permeation chromatography[10].

Shear modulus values at low temperature

Comparison of isotropic bulk polymer with low draw ratio oriented polymer. At low draw ratios there is negligible crystalline continuity and the structure can be regarded as alternating crystalline and amorphous material, the crystalline regions being highly oriented. This is the so-called parallel lamellar texture, identified by the typical two-point small angle X-ray diffraction pattern. For such samples we may therefore consider an idealized structure in which the crystalline 'c' axes are fully aligned in the extrusion direction and the 'a' and 'b' axes are randomly aligned perpendicular to the extrusion direction such that the macroscopic sample appears to be transversely isotropic.

The calculation of the longitudinal shear modulus of such a sample can readily be performed if one assumes homogeneity of either stress or strain, the results obtained being commonly referred to as the Reuss average (homogeneous stress) or Voigt average (homogeneous strain)[11]. The problem can be separated into two steps. First, an average longitudinal crystal modulus must be calculated, then this must be combined in a consistent fashion with the amorphous modulus.

The explicit equations for the average crystalline shear modulus (G_c) in terms of the crystal compliance (S_{ij}) or stiffness (C_{ij}) matrix elements are:—

Isotropic case

$$\text{Reuss} \quad G_c^{-1} = \tfrac{4}{15}(S_{11}+S_{22}+S_{33}) - \tfrac{4}{15}(S_{12}+S_{23}+S_{12}) + \tfrac{1}{5}(S_{44}+S_{55}+S_{66}) \tag{1}$$

$$\text{Voigt} \quad G_c = \tfrac{1}{15}(C_{11}+C_{22}+C_{33}) - \tfrac{1}{15}(C_{12}+C_{23}+C_{13}) + \tfrac{1}{5}(C_{44}+C_{55}+C_{66}) \tag{2}$$

Transverse isotropy

$$\text{Reuss} \quad G_c^{-1} = \tfrac{1}{2}(S_{44}+S_{55}) \tag{3}$$

$$\text{Voigt} \quad G_c = \tfrac{1}{2}(C_{44}+C_{55}) \tag{4}$$

The values of G_c calculated by the above expressions and using the theoretical S_{ij} and C_{ij} of Tadokoro *et al.*[12] are quoted in *Table 1*.

We then calculate the sample modulus G for a sample of crystallinity χ and amorphous modulus G_a using one of the following expressions:

$$\text{Reuss} \quad G^{-1} = \chi G_c^{-1} + (1-\chi G_a^{-1} \tag{5}$$

$$\text{Voigt} \quad G = \chi G_c + (1-\chi) G_a \tag{6}$$

Table 1 Summary of theoretical calculations of the shear modulus of oriented or isotropic samples, with assumed crystallinity 0.8, for different values of amorphous shear modulus. (Average crystal moduli calculated from Tadokoro *et al.*). All data in GPa

	Isotropic sample		Oriented sample	
	Reuss average	Voigt average	Reuss average	Voigt average
Average crystal shear modulus	3.08	23.5	2.15	2.4
Predicted sample moduli for				
G_a = 0.3	1.08	18.9	0.96	1.98
1	2.18	19.0	1.75	2.12
2	2.78	19.2	2.12	2.32
3	3.06	19.4	2.28	2.52

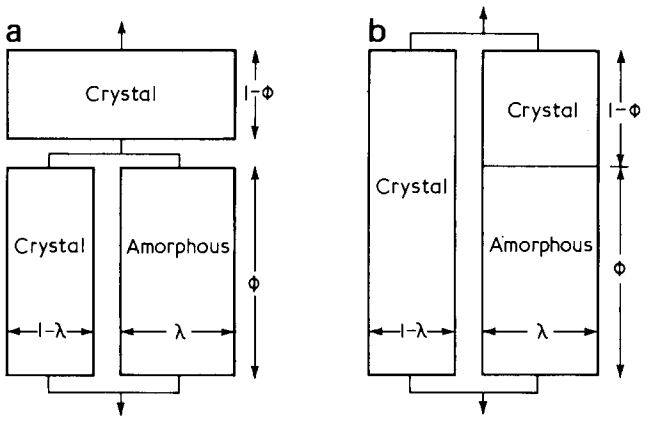

Figure 3 Modified Takayanagi models for calculation of shear or tensile moduli. (a) The Series–Parallel model, (b) the Parallel–Series model

Equations (1) or (3) are then used in combination with equation (5) and equations (2) or (4) in combination with equation (6) to obtain the Reuss and Voigt averages respectively.

Table 1 summarizes the results of these calculations for different values of G_a. We note that the theoretical values for the oriented samples are fairly similar, irrespective of whether Reuss or Voigt averaging is used and that a value ~ 1 GPa for G_a produces reasonable agreement with the observed modulus of ~ 1.8 GPa at -196°C. The predicted value for the isotropic sample is, however, critically dependent on the averaging procedure. As found in previous studies of mechanical anisotropy where shear deformations predominate, the experimental results are more in accord with the Reuss average. In view of the large difference between the Reuss and Voigt results, no reliable estimate of the amorphous shear modulus can be made except to say that a value of 1 GPa is reasonable since the observed value of 3 GPa then falls between the theoretical Reuss and Voigt bounds, being close to the Reuss bound.

Turning to the -50°C data, we find that a value of $G_a \sim 0.3$ GPa leads to Reuss average moduli of ~ 1 GPa in accordance with the observed results for both isotropic and oriented samples.

To summarize, we have shown that the similarity in the shear moduli of isotropic and oriented samples at ~ -50°C and the greater modulus of the isotropic samples at -196°C can be simply explained by taking the appropriate Reuss averages.

The higher shear modulus of the isotropic samples at low temperatures occurs because of the contribution of the stiffer modes of deformation as reflected in the terms S_{33}, C_{33} etc. in equations (1) and (2).

The increase in -50°C plateau shear modulus with increasing draw ratio

In our previous paper[1] it has been shown that the increase in tensile modulus with draw ratio for linear polyethylene can be quantitatively explained in terms of the increasing degree of crystal continuity. A model was developed which at its simplest level reduces to the Takayanagi model, although to explain the temperature dependence and obtain a precise fit to the experimental data, a more sophisticated treatment in terms of a short fibre reinforced composite is required, as will be discussed later.

We will first consider the changes in -50°C plateau modulus in terms of the Takayanagi model, shown in *Figures 3a* and *b*. The Series–Parallel arrangement gives a value for the shear modulus of the oriented polymer G_1,

$$G_1 = \left[\frac{1-\varphi}{G_c} + \frac{\varphi}{\lambda G_a + (1-\lambda)G_c}\right] \tag{7}$$

where G_c, G_a are the shear moduli of the crystalline and amorphous phases respectively and λ, φ are defined in *Figure 3a* in accordance with Takayanagi's nomenclature.

The Parallel–Series arrangement of *Figure 3b* gives a second value for the shear modulus of the oriented polymer G_2,

$$G_2 = (1-\lambda)G_c + \lambda\left[\frac{1-\varphi}{G_c} + \frac{\varphi}{G_a}\right]^{-1} \tag{8}$$

On the random crystalline bridge model the volume fraction of continuous phase v_f (termed the fibre phase by analogy with a fibre reinforced composite) is determined by calculating the weight fraction of crystalline sequences which link two or more adjacent lamellae. In our previous paper[1] it was shown that

$$v_f = \chi p(2-p) \tag{9}$$

where, as discussed above, p defines the probability that a crystalline sequence links two adjacent lamellae.

We have therefore evaluated equations (7) and (8) in terms of p and χ rather than φ and λ. This can be done by identifying v_f with $(1-\lambda)$, hence

$$1-\lambda \equiv \chi p(2-p) \tag{10}$$

and, in addition,

$$1-\varphi\lambda \equiv \chi \tag{11}$$

Equations (10) and (11) thus allow calculation of φ and λ for a given p and χ. Density, d.s.c. and broad line n.m.r. data[13,14] suggest a value for $\chi \sim 0.8$ for all samples and p has been estimated to reach values as high as 0.4 for the most highly drawn samples[1,2].

In *Table 2a* we show calculated values of G_1 and G_2 for values of G_a of 0.3 and 1 GPa, which were chosen to fit the low draw ratio results at $-50°$ and -196°C respectively. For consistency, we have taken average crystal shear moduli based on the Reuss and Voigt averaging procedures for the Series–Parallel and Parallel–Series cases respectively.

It can be seen that either calculation predicts a significant increase in -50°C plateau shear modulus with increasing crystalline continuity, although the Parallel–Series predicts the smaller absolute change which is more in agreement with the experimental data (*Table 2b*). Changes in crystalline continuity produce much smaller changes in the shear modulus for higher values of G_a (~ 1 GPa) in accordance with the observed behaviour at -196°C. Here the two calculations predict very similar values for the shear modulus and are in good agreement with the experimental data.

Prediction of the dynamic tensile deformation behaviour

As already mentioned, it has previously been shown that the tensile behaviour of these high modulus materials can be most simply considered in terms of the Takayanagi model. The structure of the materials is regarded as a

Table 2a Calculated shear moduli based on Series–Parallel model (G_1) or Parallel–Series model (G_2) for various values of p. Results are presented for G_a = 0.3 GPa and 1 GPa, corresponding to −50°C and −196°C results respectively. All moduli are quoted in GPa

	G_a = 0.3 GPa		G_a = 1 GPa	
p	G_1	G_2	G_1	G_2
0	0.96	0.96	1.75	1.75
0.1	1.36	1.11	1.82	1.80
0.2	1.55	1.25	1.87	1.85
0.3	1.67	1.39	1.91	1.90
0.4	1.75	1.53	1.95	1.94

Table 2b Experimental values for shear modulus G' (1 Hz) as a function of draw ratio at −55°C and −196°C

Draw ratio	Shear modulus	
	G' at −55°C	G' at −196°C
5.2	1.04	–
14.2	1.26	1.80
16.2	1.30	1.87
19.8	1.35	1.90
25.0	1.40	1.95

lamellar texture which is increasingly linked by crystalline bridges with increasing draw ratio. We have noted in our previous studies that the most appropriate model for the tensile behaviour is the Parallel–Series model of *Figure 3b* where the parallel crystalline element which provides the crystalline continuity consists of crystalline material which links two or more adjacent lamellae. The remaining lamellar material and non-crystalline material are considered as being in series. The rapid rise in modulus with increasing draw ratio is therefore attributed to the increase in crystalline bridge material. We have discussed in detail elsewhere[2,15] the essential equivalence of the two forms of the Takayanagi model shown in *Figures 3a* and *3b*, when allowance is made for the imperfect transmission of tensile stress caused by the finite length of the stiffening crystalline sequences.

Our previous paper was primarily concerned with establishing the relationship between the −50°C plateau modulus and the degree of crystalline continuity. In the present paper we wish to concentrate on the relaxation behaviour rather than the plateau moduli and show how this can also be understood in terms of a simple model.

The α-relaxation region

The high temperature α-relaxation is envisaged as a crystalline process involving simultaneous rotation and translation of molecular chains in both the *trans* lamellar intercrystalline bridges and the remaining lamellar (possibly chain folded) material. Although this behaviour can be represented in terms of either form of the Takayanagi model by a reduction in E_c, the modulus of the crystalline phase, it is more instructive to take up the analogy with an aligned short fibre composite. Not only does this provide a more satisfactory physical explanation of the α-relaxation process, it also expands the theory in a natural way from the one-dimensional treatments to a more general treatment capable of embracing both tensile and shear behaviour.

We have already noted that the form of the Takayanagi model shown in *Figure 3b* appears to correspond most clearly to the real situation. In the extension to the short fibre composite, the fibre phase is the parallel crystalline component and the matrix phase is the remaining mixture of lamellar and non-crystalline material. We now propose that this short fibre composite model (often called the Cox model[16]) can also provide a good basis for physical understanding of the magnitudes of the α and γ-relaxations in tensile deformation of the polymer.

Following Cox, consider a composite consisting of a parallel array of fibres of radius r_f packed in cylinders of the matrix of radius r_m (*Figure 4*). It is assumed that the energy losses depend only on shear of the matrix material. The energy loss per cycle W is then

$$W = \iiint G''_m \gamma^2_{r,x} 2\pi r \, dr \, dx \qquad (12)$$

where G''_m is the shear loss modulus of the matrix, $\gamma_{r,x}$ is the shear strain in the matrix at the point r, x; and the integral is taken over the volume of the matrix.

The essence of the Cox model is that the stress is transmitted from fibres to matrix by shear of the matrix. Application of a tensile stress to the overall composite therefore results in shear of the matrix. In a tensile experiment we represent these losses in shear in the matrix by the tensile loss modulus E'' so that

$$W = E'' e^2 \pi r_m^2 l_f \qquad (13)$$

where e is the magnitude of the tensile strain and l_f is the length of the reinforcing fibres. Hence

$$E'' = \frac{2G''_m}{r_m^2 l_f e^2} \iint \gamma^2_{r,x} \, r \, dr \, dx \qquad (14)$$

It is shown in the appendix how $\gamma_{r,x}$ may be found from the Cox model and the integral evaluated.

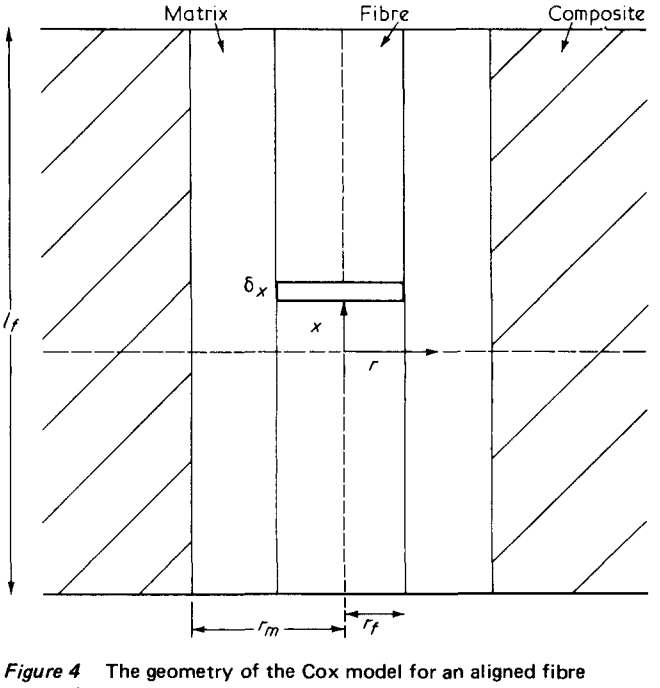

Figure 4 The geometry of the Cox model for an aligned fibre composite

We have

$$E'' = G''_m \frac{r_f^2}{r_m^2} \frac{r_f^2}{l_f^2} \left(\frac{E_f}{G'_m}\right)^2 \frac{ln(r_m/r_f)}{2} \left(\frac{\beta l_f}{2}\right) \frac{\{\sinh(\beta l_f) - \beta l_f\}}{\cosh^2(\beta l_f/2)} \quad (15)$$

where

$$\beta l_f = \left(\frac{G'_m}{E_f}\right)^{1/2} \left(\frac{l_f}{r_f}\right) \left(2\ln(r_f/r_m)\right)^{1/2}$$

The tensile storage modulus of the composite is given by the Cox formula

$$E' = E_f v_f \left(1 - \frac{\tanh \beta l_f/2}{\beta l_f/2}\right) + E_m v_m \quad (16)$$

where E_f, E_m are both considered as non-lossy; v_f, v_m are the volume fraction of fibre and matrix phase respectively.

It can be seen that the magnitude of E'' depends on geometric factors which are constant for a given structure, r_f, r_m and l_f, and on the ratio (G'_m/E_f) which will be constant for a given structure but is also temperature dependent. This ratio (G'_m/E_f) also affects the shear lag factor βl_f which determines the effectiveness of stress transfer and hence directly influences the value of E'. The absolute magnitude of the losses is also determined by (r_f/r_m), which relates directly to the volume fraction of the fibres and (l_f/r_f) which is the aspect ratio of the fibres.

In the first instance the application of the model to the high temperature regime will be considered, i.e. from the -50°C plateau upwards in temperature to include the α-relaxation. For this range of temperatures the contribution of the matrix modulus E_m to the storage modulus E' will be neglected.

As discussed above the volume fraction of fibre phase is given by

$$v_f = \chi p(2-p)$$

It is the crystalline sequences which link two or more adjacent lamellae which form the fibre phase, and in order to carry out the calculations above we require the aspect ratio of the fibres (l_f/r_f) in equations (15) and (16) above. On the crystalline bridge model there will be a distribution of aspect ratios. The calculations have however been simplified by taking the average crystal length of those sequences which link two or more adjacent lamellae. It may readily be shown that this gives

$$l_f = \left(\frac{2-p}{1-p}\right) L \quad (17)$$

where L is the long period.

There is no direct information on r_f, the radius of the crystalline bridge sequences. This is a key parameter because the aspect ratio of the fibres l_f/r_f plays a critical role in determining the shear lag factor and the magnitude of the losses. In view of this, and the uncertainty in the exact values of several of the other parameters involved we have attempted to establish that the spirit of our modelling is satisfactory, rather than attempting a detailed fit which would inevitably involve arbitrary adjustment of such parameters.

The shear modulus of the matrix phase and its temperature dependence were not known. We therefore proceeded by taking values of G'_m and G''_m from the experimental data for isotropic linear polyethylene. The calculations were performed on the basis of equations (15) and (16) for different values of p, which as we have seen determines $v_f = \left(\frac{r_f}{r_m}\right)^2$ and also l_f. The calculations were carried out for three different values of r_f; 10, 15 and 20 Å. Several factors were taken to have fixed values throughout all the calculations. These are (i) the volume fraction crystallinity χ, for which a value of 0.8 was chosen as above; (ii) the long period L, which was taken as 200 Å which is close to the mean value obtained from small angle measurements; (iii) a fixed value for E_f as the crystal modulus of linear polyethylene. A value of 315 GPa, based on the recent work by Tadokoro and coworkers[12] was taken for E_f which was assumed to be temperature independent.

It was found that the best overall match between the predicted and observed patterns of mechanical behaviour for both E' and $\tan\delta = E''/E'$ was obtained for $r_f = 15$ Å. These results are shown in *Figures 5a* and *5b* and may be compared with the experimental results shown in *Figures 6a* and *6b*. These are two aspects of the correspondence between the predicted and experimental values which can be highlighted. First, the modelling does predict the correct magnitudes for the -50°C plateau moduli and in particular the increase in plateau moduli with increasing p as the draw ratio increases. Note that a p value of 0.4 (which is achieved for draw ratio $\sim$25) gives a plateau modulus value $\sim$100 GPa. Secondly, the fall in E' with temperature is modelled quite well, and in particular, the magnitude of the fall with temperature decreases with increasing p, as is observed. Tan δ_E for the α relaxation is predicted to fall as p increases, which is consistent with the observed behaviour. In this respect it may readily be shown from equations (15) and (16) that for high crystalline continuity where there is good stress transmission

$$\tan\delta_E = \frac{E''}{E'} \rightarrow \frac{\tan\delta_G}{\beta l_f}$$

and therefore falls with increasing βl_f. This result is physically reasonable, as in the limit of perfect stress transmission there is uniform tensile strain and no inhomogeneous shear. We therefore see that in this model, the α relaxation process is a consequence of shear in the crystalline regions of the matrix.

In the present calculations, the predicted curves were obtained with values for some of the parameters which differ from those which we adopted in our previous paper where we were concerned only with prediction of the -50°C plateau moduli. In the present paper a value of χ of 0.8 was chosen and the predicted curves of *Figures 5a* and *5b* imply an average shear lag factor

$$\varphi' = 1 - \frac{\tanh \beta l_f/2}{\beta l_f/2}$$

at -50°C of about 0.8. In our previous paper it was pointed out that the numerical fits were complicated by the problem of choosing realistic crystallinity values for the samples. However, in that paper we were primarily concerned with showing that the large increase in modulus with draw ratio could be attributed to the large increase in the factor $p(2-p)$. It was only necessary to

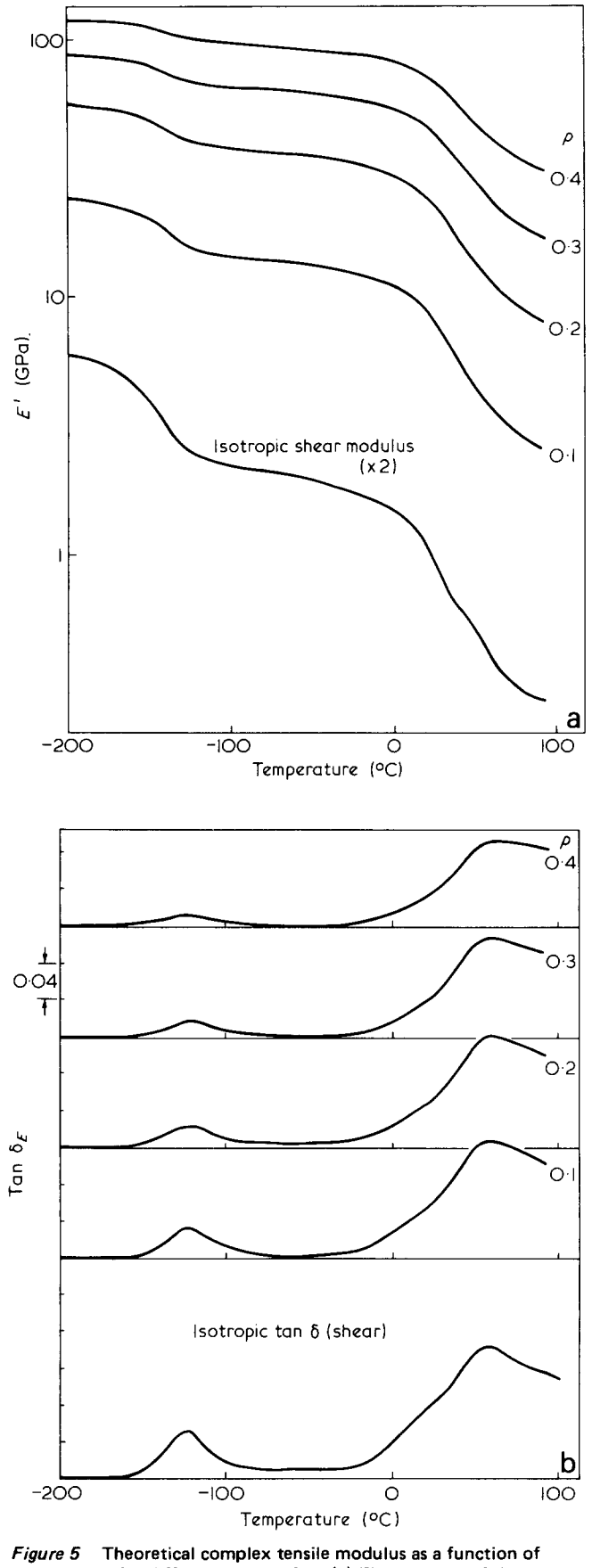

Figure 5 Theoretical complex tensile modulus as a function of temperature for different values of p. (a) The real part of the modulus E'. (b) Tan δ_E (tensile). (The isotropic sample data which were used for the matrix shear modulus are also shown)

assume that the product $\chi\varphi'$ was 0.6 to give a good numerical fit to the -50°C plateau moduli. In the present paper, to give a realistic temperature dependence for G' as well as a reasonable numerical fit to the -50°C moduli, it was necessary to choose φ' at -50°C with a value of ~ 0.8. It should also be remarked that a value of $E_c = 315$ GPa has been chosen in this paper compared with 255 GPa in

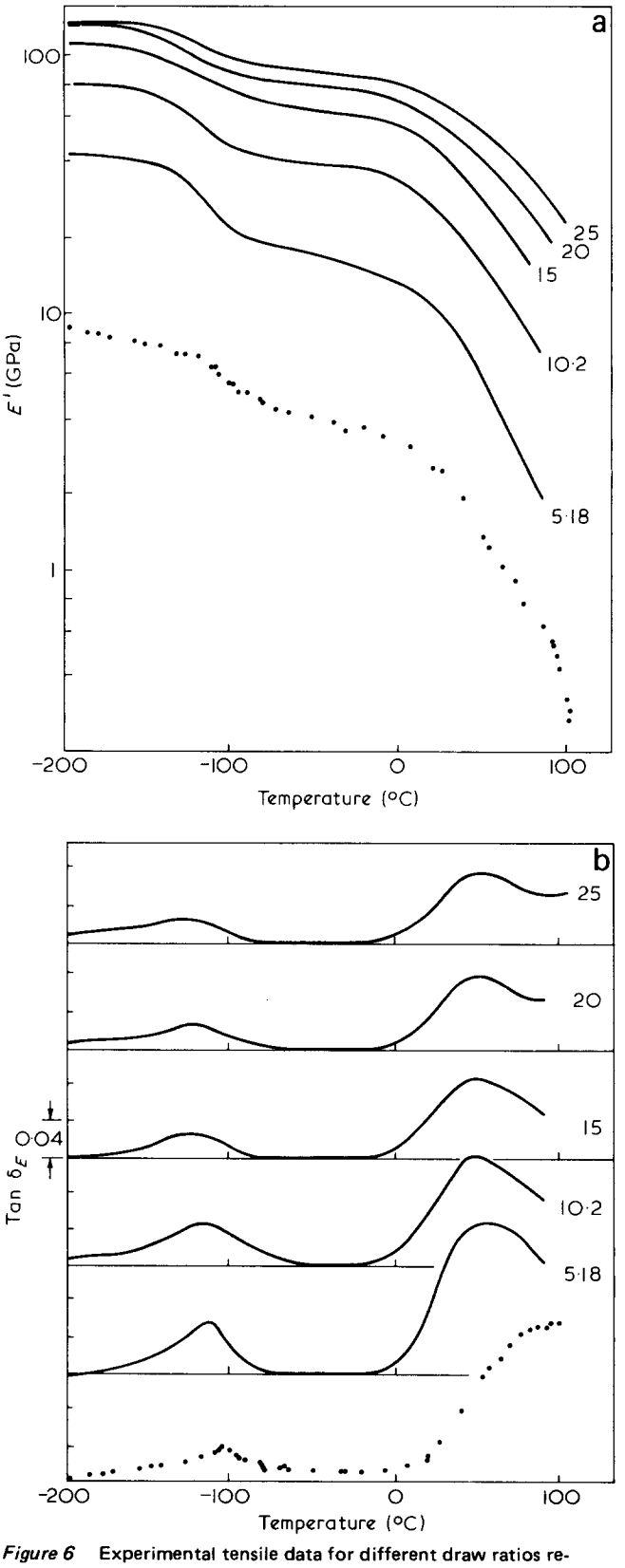

Figure 6 Experimental tensile data for different draw ratios reproduced from ref 1. (Experimental points shown for isotropic sample only). (a) Real part of the modulus E'. (b) Tan δ_E

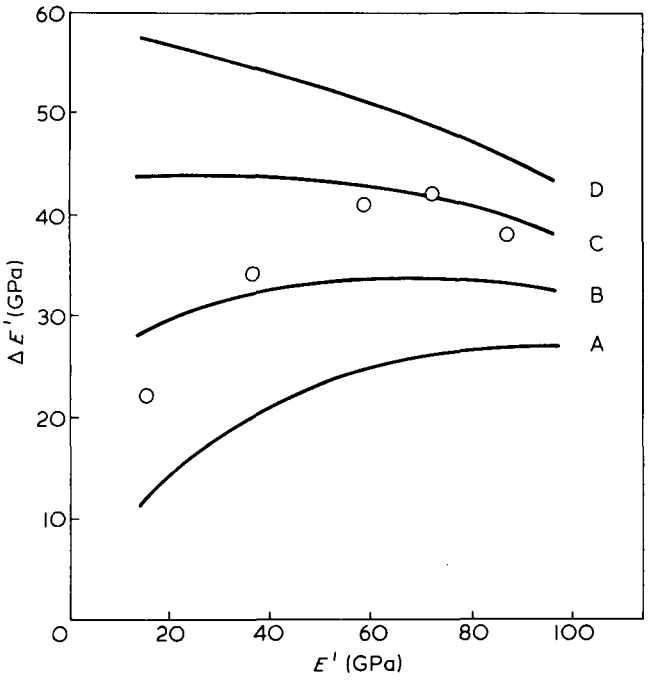

Figure 7 The increment in modulus (ΔE) between −50°C and −196°C as a function of the modulus at −50°C. Points are experimental data. Lines A → D represent the predictions of equation (16) with E_a = 0, 5, 10, 15 GPa

the previous paper. In view of recent developments it appeared most appropriate to take the recent value for the crystal modulus.

The γ relaxation region

Finally, we wish to consider the temperature region below −50°C. There will be an increase in modulus with decreasing temperature for two reasons. First, the shear lag factor will increase due to the increase in G'_m. Secondly, the second term in equation (16) will become important, as E_m increases in value. It is instructive to examine the contribution from these two factors by adopting the following procedure. We denote by ΔE the difference between the value of the tensile modulus at the −50°C plateau and its value at −196°C. First consider the value for ΔE calculated on the basis of equation (16) using the parameters for the predictions of *Figure 5a*, but ignoring the matrix contribution term $E_m v_m$. This gives a shear lag contribution to ΔE which is shown in *Figure 7* as a function of the −50°C plateau modulus obtained from the same calculation (Line A). It can be seen that this contribution is not sufficient to account for the observed increase in modulus with decreasing temperature, and we must conclude that the term $E_m v_m$ is significantly large.

The matrix tensile modulus E_m can be estimated on the basis that the matrix phase consists of a mixture of and non-crystalline ('amorphous') material which are considered to be in series. Denoting the modulus of the amorphous material by E_a we have

$$\frac{\chi(1-p)^2+(1-\chi)}{E_m}=\frac{\chi(1-p)^2}{E_c}+\frac{(1-\chi)}{E_a} \qquad (18)$$

In addition to the increase in E_m due to the increase in E_a at low temperatures, we also have to consider the change in the volume fraction of the matrix $v_m=(1-v_f)$ as the crystal continuity changes with increasing draw ratio. Both of these factors change the value of the matrix contribution term $E_m v_m$. In *Figure 7* we show calculated curves for ΔE as a function of the −50°C plateau modulus (which varies with crystal continuity on the draw ratio changes) for three values of E_a at −196°C, 5, 10 and 15 GPa. It can be seen that the experimental data cut across these predicted curves, suggesting that E_a increases as the −50°C plateau modulus increases, i.e. as the draw ratio increases. It appears that low draw ratio samples have values for $E_a \sim 3$ GPa, whereas the high draw samples show $E_a \sim 10$ GPa. Such values would appear realistic in terms of an increasing degree of amorphous orientation with increasing draw ratio, and are in line with modulus values for oriented amorphous polymers[17]. In this connection it is worth noting that the simple Takayanagi Parallel–Series model with no shear lag factor at −50°C would require values for E_a at −196°C of ~15 GPa (based on $E_c = 315$ GPa).

CONCLUSIONS

(1) The cross-over in shear modulus for isotropic and oriented samples in the temperature region of the γ-relaxation has been explained in terms of Reuss and Voigt averaging procedures.

(2) The increase in the −50°C plateau shear modulus with increasing draw ratio can be predicted by Takayanagi models, on the basis of the increasing degree of crystal continuity.

(3) The temperature dependence of the dynamic mechanical tensile behaviour has been satisfactorily modelled by a simple extension of the Cox short fibre composite model. For the α-relaxation, the modelling predicts the correct magnitudes for the −50°C plateau moduli, the fall in E' with temperature and the fall in tan δ_E with increasing crystal continuity.

(4) In the case of the γ relaxation, it appears that there are two mechanisms for the change in modulus and hence for tan δ_E. The first is an increase in the efficiency of stress transfer with falling temperature due to quenching of molecular motions. These are probably predominantly if not entirely in the non-crystalline regions. Secondly, the quenching of these molecular motions also gives rise to an increase in the stiffness of the non-crystalline regions, which then contribute directly to the overall stiffness of the sample.

REFERENCES

1 Gibson, A. G., Davies, G. R. and Ward, I. M. *Polymer* 1978, **19**, 683
2 Gibson, A. G., Davies, G. R. and Ward, I. M. *Polym. Eng. Sci.* 1980, **20**, 941
3 Gibson, A. G. and Ward, I. M. *J. Mater. Sci.* 1979, **14**, 1838
4 Gibson, A. G., Greig, D. and Ward, I. M. *J. Polym. Sci., Polym. Phys. Edn.* 1980, **18**, 1481
5 Gibson, A. G. and Ward, I. M. *J. Polym. Sci., Polym. Phys. Edn.* 1978, **16**, 2015
6 Clements, J., Jakeways, R. and Ward, I. M. *Polymer* 1978, **19**, 639
7 Heijboer, J., Dekking, P. and Staverman, A. J. Proc. End. Int. Cong. Rheology (Ed. V. G. W. Harrison), Butterworths, London, 1954, p. 123
8 Folkes, M. J. and Arridge, R. G. C. *J. Phys. D. Appl. Phys.* 1975, **8**, 1053
9 Frye, C. J., Ward, I. M., Dobb, M. G. and Johnson, D. J. *Polymer* 1979, **20**, 1310
10 Capaccio, G. and Ward, I. M. *J. Polym. Sci., Polym. Phys. Edn.* 1981, **19**, 667

11 Ward, I. M. 'Mechanical Properties of Solid Polymers', Wiley, London, 1971, p. 254
12 Tashino, K., Kobayashi, M. and Tadokoro, H. *Macromolecules* 1978, **11**, 914
13 Clements, J., Capaccio, G. and Ward, I. M. *J. Polym. Sci., Polym. Phys. Edn.* 1979, **17**, 693
14 Smith, J. B., Manuel, A. J. and Ward, I. M. *Polymer* 1975, **16**, 57
15 Gibson, A. G., Holt, J. S. and Hope, P. S. *J. Polym. Sci., Polym. Phys. Edn.* 1979, **17**, 1375
16 Cox, H. L. *J. Appl. Phys.* 1952, **3**, 72
17 Ward, I, M., Ed. 'Structure and Properties of Oriented Polymers', Applied Science Publishers Ltd., London, 1975, p. 319
18 McLean, D. and Read, B. E. *J. Mater. Sci.* 1975, **10**, 481

APPENDIX

This appendix outlines the calculation of the complex tensile modulus of an aligned fibre reinforced composite with a lossy matrix, in the general spirit of the Cox model. Since this paper was submitted for publication a previous attempt to determine the storage and loss moduli of short fibre reinforced composites by McLean and Read[18] has been pointed out to us. Although this appendix repeats part of these earlier treatments we believe that this is necessary if our treatment, which differs from that of McLean and Read, is to be made clear to the reader.

We first briefly consider the derivation of the tensile modulus of a non-lossy composite. The essential assumptions are that the tensile stress in the matrix is negligible and that the shear stress at the surface of the fibres may be calculated by considering the idealized model shown in *Figure 4*. This represents a fibre of length l_f and a radius r_f surrounded by a cylinder of matrix material of radius r_m chosen such that $1/\pi r_m^2$ is the average number of fibres per unit cross sectional area of composite. At this radius it is assumed that the tensile strain in the matrix is equal to the applied strain in the composite. Within this radius, however, the strain is non uniform, depending both upon x and r although it is assumed that strain in the fibre depends only upon x.

Consider the change in total tensile load (P) carried by the fibre between x and $x+\delta x$. This must be equal to the total force applied by the shear stress (τ) in the matrix at the surface of the fibre, i.e.

$$\delta P = -2\pi r_f \delta x \tau(r_f,x)$$

or

$$\frac{dP}{dx} = -2\pi r_f \tau(r_f,x) \tag{1A}$$

In order to integrate this equation to determine the average load borne by the fibre we must solve for $\tau(r_f,x)$. To do this, we introduce the variable $\omega(r,x)$ which represents the vertical displacement of any point in the matrix. $\left(\frac{\partial\omega}{\partial r}\right.$ is then the shear strain in the matrix.$\left.\right)$ Hence, if G_m is the matrix shear modulus

$$\tau = \frac{\partial\omega}{\partial r}\cdot G_m \tag{2A}$$

Also, considering the vertical equilibrium of a thin disc of material, extending from the surface of the fibre at $r=r_f$ to the general point r, if tensile stresses in the matrix are to be ignored we must have:

$$2\pi r\,\tau(r,x) = 2\pi r_f\,\tau(r_f,x) \tag{3A}$$

Hence

$$\frac{\partial\omega}{\partial r} = \frac{\tau(r_f,x)}{G_m}\cdot\frac{r_f}{r} \tag{4A}$$

and integrating the above equation between r_f and r_m we obtain:

$$\Delta\omega = \frac{r_f\tau(r_f,x)}{G_m}\ln(r_m/r_f) \tag{5A}$$

If the vertical displacement of the matrix at $r=r_f$ is U and at $r=r_m$ is V then $\Delta\omega = V-U$ and the above equation becomes

$$\tau(r_f,x) = G_m(V-U)/(r_f\ln(r_m/r_f)) \tag{6A}$$

substituting in equation (1A) we therefore obtain

$$\frac{dP}{dx} = 2\pi G_m(V-U)/\ln(r_m/r_f) \tag{7A}$$

Hence, by differentiation,

$$\frac{d^2P}{dx^2} = -2\pi G_m\left(\frac{dV}{dx}-\frac{dU}{dx}\right)/\ln(r_m/r_f) \tag{8A}$$

We note that $\frac{dV}{dx}$ is the tensile strain in the matrix at $r=r_m$ which is assumed to be equal to the applied strain e. Also, if we assume perfect bonding between fibre and matrix then $\frac{dU}{dx}$, the matrix strain at $r=r_f$, is equal to the strain in the fibre e_f. This may be expressed in terms of P, r_f and E_f, the tensile modulus of the fibre:

$$\frac{dU}{dx} = e_f = P/(E_f\pi r_f^2) \tag{9A}$$

Hence, equation (8A) becomes:

$$\frac{d^2P}{dx^2} = 2\pi G_m\left[\frac{P}{E_f\pi r_f^2}-e\right]/\ln(r_m/r_f) \tag{10A}$$

If it is assumed that no load is directly transmitted across the ends of the fibre then $P=0$ at $x=\pm l_f/2$. The solution of the above equation then becomes:

$$P = eE_f\pi r_f^2\left(1-\frac{\cosh(\beta x)}{\cosh(\beta l_f/2)}\right) \tag{11A}$$

where

$$\beta = \left[\frac{2}{r_f^2\ln(r_m/r_f)}\cdot\left(\frac{G_m}{E_f}\right)\right]^{1/2}$$

and the mean stress in the fibre $\bar{\sigma}$ is given by

$$\bar{\sigma}_f = \frac{1}{l_f}\int_{-l_f/2}^{l_f/2}\frac{P}{\pi r_f^2}dx = \frac{eE_f}{l_f}\int_{-l_f/2}^{l_f/2}\left(1-\frac{\cosh(\beta x)}{\cosh(\beta l_f/2)}\right)dx \tag{12A}$$

This integrates to give

$$\bar{\sigma}_f = E_f e\left(1-\frac{\tanh(\beta l_f/2)}{\beta l_f/2}\right) \tag{13A}$$

Since there is no tensile stress in the matrix, the average stress σ over the cylinder of radius r_m is given by $V_f \bar{\sigma}_f$ where V_f is the volume fraction of the fibres. The apparent tensile modulus E is therefore given by:

$$E = \frac{\sigma}{e} = V_f \frac{\bar{\sigma}_f}{e} \tag{14A}$$

or

$$E = V_f E_f \left(1 - \frac{\tanh(\beta l_f/2)}{\beta l_f/2}\right) \tag{15A}$$

Some account may be taken of the tensile stress in the matrix if we include the term $V_m E_m$ in the above equation where V_m is the volume fraction of the matrix and E_m is its tensile modulus. This then yields the equation quoted in the main text.

We note that for efficient reinforcing action $\beta l_f \gg 1$ which is obtained with high densities of high aspect ratio fibres in a matrix with a high shear modulus.

To extend this analysis to deal with a lossy matrix we make the basic assumption that all the energy dissipation occurs as a result of the shear deformation in the matrix phase. As noted in the text, if G''_m is the imaginary part of the matrix shear modulus, then the energy loss per cycle (W) is given by:

$$W = \int_{-l_f/2}^{l_f/2} \int_{r_f}^{r_m} G''_m \gamma^2 2\pi r \, dr \, dx \tag{16A}$$

where γ is the shear strain in the matrix at the point (r,x).

In a tensile experiment, however, one would interpret this energy loss as the imaginary part of the tensile modulus of the composite (E''). Hence

$$W = E'' e^2 \pi r_m^2 l_f \tag{17A}$$

Equating equations (16A) and (Z7A) yields

$$E'' = \frac{2G''_m}{r_m^2 l_f} \int_{-l_f/2}^{l_f/2} \int_{r_f}^{r_m} \left(\frac{\gamma}{e}\right)^2 r \, dr \, dx \tag{18A}$$

The previous calculation may be extended to provide the ratio of shear strain to the applied tensile strain by differentiating the solution for P (equation (11A)). This yields

$$\frac{dP}{dx} = -eE_f \pi r_f^2 \beta \frac{\sinh(\beta x)}{\cosh(\beta l_f/2)} \tag{19A}$$

Substituting from equations (1A) and (3A) we have

$$2\pi r \tau(r,x = e E_f \pi r_f^2 \beta \frac{\sinh(\beta x)}{\cosh(\beta l_f/2)} \tag{20A}$$

The shear strain γ is simply the shear stress τ divided by the matrix shear modulus. Hence:

$$\frac{\gamma}{e} = \frac{E_f r_f^2}{2G_m} \cdot \frac{\beta}{\cosh(\beta l_f/2)} \cdot \frac{\sinh(\beta x)}{r} \tag{21A}$$

This is essentially the expression which we require to substitute into the integral of equation (18A). Note, however, that we are now dealing with a viscoelastic system and that the ratio required in equation (18A) is that of the absolute magnitude of the shear and tensile strains. We compute this from equation (21A) by considering only the real part of the matrix shear modulus (i.e. we equate G_m with G'_m). This is an acceptable procedure for small loss angles.

The full expression for E'' therefore becomes

$$E'' = \frac{2G'_m}{r_m^2 l_f} \cdot \left(\frac{E_f r_f^2}{2G'_m}\right)^2 \cdot \frac{\beta^2}{\cosh^2(\beta l_f/2)} \int_{-l_f/2}^{l_f/2} \int_{r_f}^{r_m} \frac{\sinh^2(\beta x)}{r} dr \, dx \tag{22A}$$

This may be integrated to give the result quoted in the main text.

This approach differs fundamentally from that of McLean and Read in that the loss mechanism is specifically assumed to be associated with the shear deformation of the matrix and is not associated with its tensile properties. We believe this to be an important distinction since the matrix in our case consists of aligned crystalline and amorphous material and, certainly in the case of α_c relaxation, we believe this to be a crystalline shear process.